Decentralized Smart Energy Systems

Erasmus Mundus Joint Master Degree

University of Lorraine

Green Energy Buildings

Challenge Based Module

Supervised by:

1. Eugenio Schillaci
2. David Lacroix
3. Gilles Pernot
4. Christel Metivier

Team members:

1. Abir Saha
2. Andrea Eka Putri
3. Jose Andrés Santamaría Cordero
4. Rajnesh Kumar
5. Sara-Medina Šehović

June 2024

Table of Contents

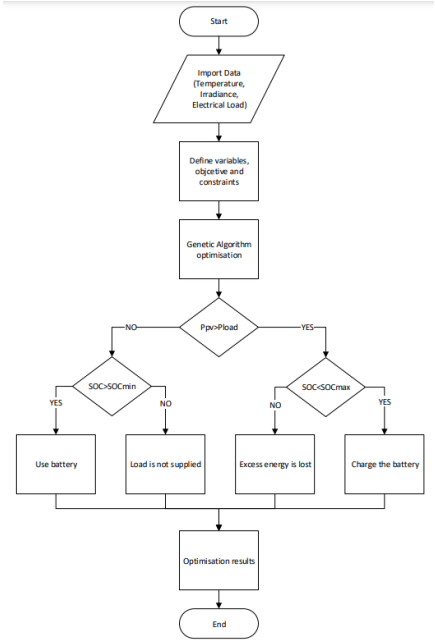

List of Figures

List of Tables

No table of figures entries found.

Glossary

XX	XXX

Executive Summary

[unfinished]

With the rise of cooling -> effort has to be made to lower the hvac load. By implementing green energy building

It is required to get data as close as how the building reacts -> deswegen we need the 1D, that's our main objective.

Then followed by the choosing of the energy production plant. Investigation with respect to economic and environment was made. Eventually, the pv with grid connected system is chosen with the value LCOE of xxx and payback period of xxx.

Introduction

Problem Statement

The International Energy Agency on their report *The Future of Cooling* [1] mentioned that energy demand for space cooling and heating will increase by more than triple in 2050, where it will contribute up to 49% of all energy demand. The problem is even amplified with the rising of income and population in the world's hotter regions, where most homes in those areas have not yet purchased their first Air Conditioner (AC). AC sales is expected to increase rapidly in emerging economies such as China, Indonesia and India, where together account for the half of the total AC stock by 2050. Figures of the trends are attached in Appendix A.

Efforts must be made to reduce the overall energy consumption coming from Heating, Ventilation, and Air Conditioning (HVAC) system, while simultaneously guaranteeing required room comfort conditions. Achieving this balance is important to enhance energy efficiency and sustainability in office buildings. With that being said, one of the approaches is the implementation of green building features.

Various simulations are conducted to analyze the effectiveness of the green building features in reducing the HVAC load, utilizing zero-dimensional (0D) and one-dimensional (1D) modelling techniques. Simulations with 0D and 1D modelling offer valuable insights into the heat flows occurring in the building. The 0D model will offer a macro-level perspective, while 1D model offers insights on the interactions between the rooms.

Objectives

From the problem stated above, three objectives are introduced for the Challenge-Based Module of Green Energy Buildings:

1. To build a 0D and 1D numerical model to track the temperature evolution along the year and thermal gains and losses.
2. To compare the differences between 0D and 1D analysis results to determine the effectivity.
3. To perform calculation of the HVAC system needed for the building with the impact of green building features.
4. To select the energy production plant by using thermo-economic and technical-environmental assessment.

Building Specifications

The investigation will be based on an office building located in Terrassa, Barcelona with a coordinate of 41°33'49"N 2°01'23"E. The average temperature on the area is ranging from 9° C in winter to 29° C in summer [2]. The building has 14 sections with 8 office rooms (highlighted in green on Figure 2), 3 other functional rooms (blue), and 2 non-conditioned areas (red). Each office room is designed to accommodate 3 occupants, each equipped with a computer.

The building involves various materials utilized in the walls, roof, or floor. The specific materials have previously mentioned in the topic description and building dimensions were measured from the provided AutoCAD files. For the purpose of this study, all relevant dimensions and materials properties have been compiled in Appendix A, which will be used for further calculations.

The building involves various materials utilized in the walls, roof, or floor. The specific materials have previously mentioned in the topic description and building dimensions were measured from the provided AutoCAD files. For the purpose of this study, all relevant dimensions and materials properties have been compiled in Appendix A, which will be used for further calculations.

Figure 1 Top view of the Building [3]

Figure 2 Building Plan [4]

0D and 1D Analysis

0D modelling

To perform the building modelling in 0D a single control volume consisting of the whole building was considered. The general energy balance that was applied to the control volume, the procedure and methodology for each one of the heat transfer modes, and the time discretization The following general energy balance was applied to the control volume:

$$C\frac{\partial T}{\partial t} = Q_c + Q_v + Q_r + Q_{int} \qquad \textit{Equation 1}$$

Where,
C= Building capacitance
Q_c= Heat transfer due to conduction/convection
Q_v= Heat transfer due to ventilation
Q_{int}= Heat transfer due to internal sources inside the control volume

From this energy balance the different terms were calculated, starting with capacitance that was defined as a sum per each of the materials constituting the building, including air, glass, insulations, brick, etc., using the following equation:

$$C = \sum \rho\, c_p\, V \qquad \textit{Equation 2}$$

Where,
ρ = Density
c_p = Specific heat
V = Volume

Following, the term for conduction/convection was calculated, as a sum per wall, using the set of equations explained below. For this project a value for R_{si} of 0.13 m²/K W for standing walls, 0.17 m²/K W for the roof, 0.10 m²/K W for the floor and a value for R_{se} of 0.04 m²/K W were selected based on the surface orientation and heat flow direction [5]. Furthermore, to consider thermal bridges and junctions impact a factor of 10 % was applied to the final thermal transmittance value U [6].

$$Q_c = (T_{ext} - T_{int}) \sum U\ A \qquad \textit{Equation 3}$$

$$U = \frac{1}{R_{total}}$$

$$R_{total} = R_{si} + \sum_j \frac{L_j}{\lambda_j} + R_{se} \qquad \textit{j, sum per layer}$$

Where,

U = Thermal transmittance
A = Surface area
R = Thermal resistance
L_j = Layer thickness
λ_j = Thermal conductivity

Afterwards the heat transfer contribution due to ventilation was calculated. For this report, a value for n of 0.35 air shifts per hour was selected [7]:

$$Q_v = c_p\ \rho\ V\ n\ (T_{ext} - T_{int}) \qquad \textit{Equation 4}$$

Where,

n= Number of air shifts per second

Subsequently the heat transfer contribution due to radiation was computed using the set of equations explained below.

$$Q_r = f_{sh}\ A_{sun}\ G_{sun} \qquad \textit{Equation 5}$$

$$A_{sun} = \tau\ A_{glazed}(1 - f_f(t)\ ) \qquad \textit{For glazed surfaces}$$

$$A_{sun} = \alpha\ R_{se} U\ A \qquad \textit{For opaque surfaces}$$

Where,

f_{sh} = Shading factor
G_{sun} = Solar irradiance
τ = Transmittance
$f_f(t)$ = Reduction factor due to façades or movable curtains
α = Absorptance

For this for, a shading factor f_{sh} of 1 was considered for the building, as it is in the top floor with no surrounding taller buildings, trees or any shading. For the solar irradiance, each wall of the building was considered to have a different radiation profile across each hour of the day and across each day of the year. This profile depends on the slope and azimuth of each wall. Table 1 shows a summary of these values for each wall based on the building location and inclination with respect to the north. Based on this data the profiles for each wall were computed using the photovoltaic geographical information system of the European Union Commission [8]. Figure 3 below shows the average of each day of January and July as an example of the behavior of the irradiance. Finally, for the reduction factor due to facades and movable curtains a changing value of 0.24 in winter to 0.6 in summer was selected [9].

Table 1. Slope and Azimuth for the building walls to determine irradiation profiles

Surface	Slope [°]	Azimuth [°]
Roof	0	0
North wall	90	150
South wall	90	-30
East wall	90	-120
West wall	90	60

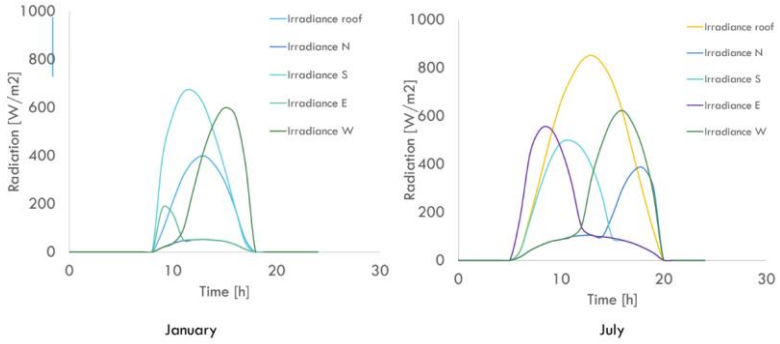

Figure 3. Irradiance profile for each building wall on the average day of January (left) and July (right)

To finish with the energy balance equation, the heat transfer contribution due to internal sources was computed using the equations below. For the number of people and equipment, both were considered as 3 per office and they were only active during the working hours of the building, between 8 h and 19 h. For the amount of heat, it was selected a value of 100 W for an average person in a conditioned office building and 55 W per each computer.

$$Q_{int} = \#_{people}\, Q_{person} + \#_{equip}\, Q_{equip} \qquad \textit{Equation 6}$$

Finally, using *Equation 1* with all the explained methodology a time discretization was performed using MATLAB. Forward Euler Explicit Approach was followed to determine the temperature in the next time step by using the following equation. The boundary conditions for initial temperature were determined by iteration as averages on the steady state temperature of the building for each month of the year after computing the results with an average of the external temperature as initial conditions. A time step (Δt) of 15 minutes was used for the time discretization. This value was obtained through a sensitivity analysis, where the obtained results of 1 second, 1 minute, 10 minutes, etc. were compared. It was noticed that if a bigger value of time step was chosen, specifically at the 1 h value, it starts influencing the results. Thus, a time step of 15 minutes was chosen as a sensible value.

$$T^{n+1} = T^n + \frac{\Delta t}{C}\left[Q_c + Q_v + Q_r + Q_{int}\right] \qquad \textit{Equation 7}$$

0D results

By applying the methodology previously explained for the OD model the temperature response of the building through time can be obtained, as shown in Figure 4. The outside temperature is also shown as a reference. For a more detailed analysis, the results are shown for the average day on

the month of July. It can be seen how the building temperature ranges approximately from 27 °C to 36 °C. When understanding this temperature range, it is important to recall that the results are based on an unconditioned building, with no HVAC system application or heat management solution has been applied. It can also be seen that the temperature of the building follows the trend of the outside temperature with some delay. This phenomenon is expected as the entire building has a significant capacitance, therefore it tends to store heat. With this reason, it could be obtained that the outside temperature peaks at around 14 h and the building temperature around 17 h.

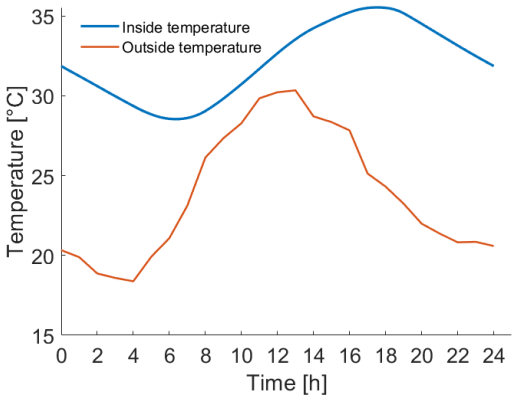

Figure 4 Temperature evolution of the building for an average day in the month of July for the 0D model

As shown, the building exhibits a temperature that's higher than the outside, this could be explained by how the heat is transferred in the building, using Figure 5. It can be seen that between multiple types of heat transfer modes, radiation is the main heat transfer with a positive contribution. This is due to the fact that most walls of the building constitute of glass materials, allowing the sun radiation to enter easily. It can also be seen that the only negative contributions, meaning the ones that are extracting heat to the outside of the building, are the ventilation and the conduction-convection. These contributions are in an absolute value comparison lower than the radiation contribution, explaining the higher temperatures inside of the building. Finally, the effect of the radiation profiles for the different walls can be observed when looking at the heat transfer distribution per wall. For example, the roof profile has a normal distribution profile with its peak around noon, while the east wall has its peak in the morning and the west wall in the afternoon. The roof is one of the biggest contributors to heat transfer into the building.

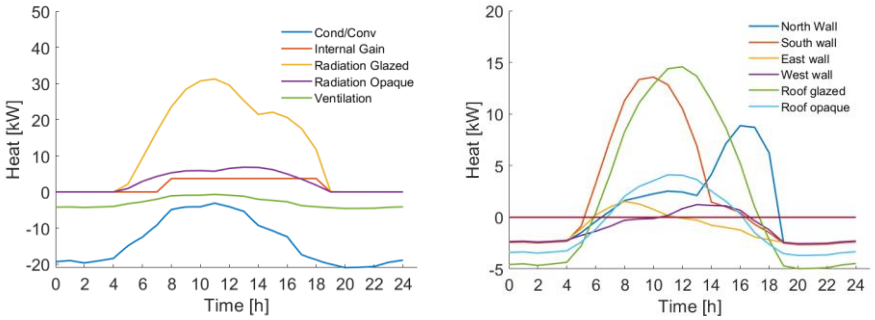

Figure 5 Heat transfer per heat mode (left) and per building wall (right) for the 0D model on the average day of the month of July

The results for the whole year of the 0D model are shown below in Figure 6. The temperature throughout the year ranges between 10 °C and 36 °C. This showcases the necessity of applying an HVAC system in the building both for heating during winter and for cooling during summer. Also, due to the combined effects of capacitance, insulation, and the contribution from radiation, it can be seen the temperature is higher in the inside of the building with respect to the outside across the entire year.

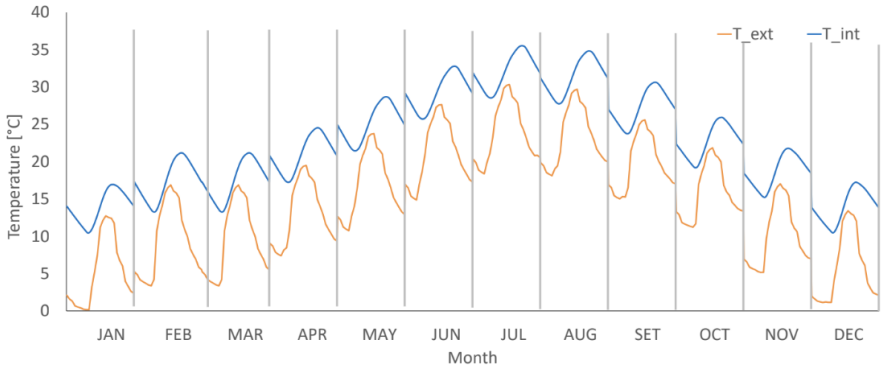

Figure 6 Temperature evolution of the building throughout the whole year for the 0D model

1D modeling

The approach for modelling in 1D is kept the same in comparison with the 0D model, with the difference that this time, there will be many other small control volumes, as opposed to just one. More specifically, the building will be divided into 14 different control volumes, each one with its own material properties, specific functions, and particularities, like unconditioned rooms, as shown in Figure 7. Therefore, for each one of the rooms the energy balance equation will be solved. Since the conduction/convection has an impact on the neighbouring control volume, all control volumes will depend on each other for the same time step and must be solved simultaneously. The energy balance discretization solved in MATLAB for a room *w* with adjacent rooms *j* and with *i* surfaces is shown in the equation below.

Figure 7 Control volumes and room distributions for 1D modelling

$$T^{n+1}{}_w = T^n{}_w + \frac{\Delta t}{C_w}\left[\sum_i U_i\, A_i\, (T_{ext} - T^n{}_w) + \sum_j U_j\, A_j\, (T^n{}_j - T^n{}_w) + \sum_i Q_{rad,i} + Q_{int,w}\right]$$

Equation 8

1D results

After applying the methodology previously described, results for the 1D model can be obtained. As it is difficult to put across data for 14 different rooms in a single plot, the use of a heat map changing with respect to the time of the day was chosen as a visualization aid and can be seen in Figure 8 below. Room temperature is usually lower at the start of the day and it rises as the sun rises and starts to heat up the building. In the afternoon, a peak temperature is achieved and then the building starts cooling down again. A delay with respect to the outside temperature is also seen in the 1D model due to the effect of capacitance.

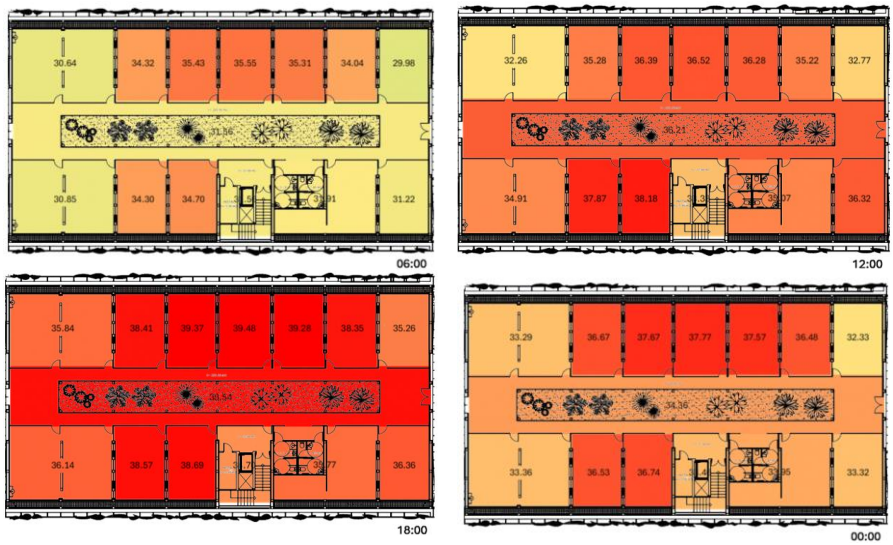

Figure 8. Evolution of temperature throughout the average day of July as a room heat map using the 1D model

Furthermore, an heterogenous behaviour can be seen across the heat map when analysing the rooms separately. This behaviour occurs as each specific rooms have different properties. One example of this are the corner rooms, which have a brick wall on each side. The effect of this brick wall, which possess a lower absorptance in relation to the glass transmittance, causes a lower heat transfer through radiation in these walls and results in a lower temperature. Another example is found with room number 12, the staircase of the building that is non-conditioned and also fully surrounded by brick walls, causing the same effect of a reduced temperature and also affecting adjacent rooms. Finally, as the sun progresses and changes position through the day, all radiation profiles that were considered for all the different rooms contribute to this heterogeneity.

0D vs 1D Comparison based on temperature

Addressing one of the main objectives of this work, a comparison between the 0D and the 1D model results was carried out. The two most important metrics to perform this comparison are temperature and HVAC load, both will be analyzed in this section.

Firstly, when considering temperature, a direct comparison between 0D and 1D could not be straightforwardly done as the 0D model possesses a single temperature but on the other hand the 1D model produces a temperature profile. This temperature profile, which as discussed previously, is highly heterogeneous between rooms. Since the final goal is to estimate HVAC load for the power plant dimensioning, the metrics of coldest room (for winter) and the average temperature of conditioned rooms were selected. In this way, a comparison of representative temperatures that are important contributors to the final metric of determining the HVAC load could be performed. The results of comparing this metrics against the 0D model temperature can be seen in Figure 9 below.

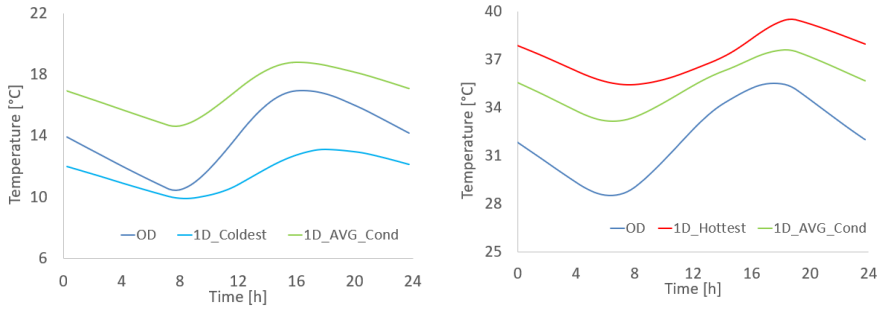

Figure 9. 0D vs 1D model temperature comparison for January (left) and July (right)

It can be seen, for example in January, that the 0D model is neither tracking the temperature of the coldest nor the average of conditioned rooms. Even though the behavior of all three curves is similar: dropping at the beginning of the day, then sometime after the sun rises so does temperature, and finally dropping again some hours after sunset, the differences in temperature are significant, even reaching around 5 °C for the most different points. When comparing the 0D model temperature to the average temperature of all conditioned rooms for example, a maximum difference of around 28 % and an average difference through the 24 h of 18 % were obtained. The same occurs in July, where a maximum difference of 14 % and an average of 10 % can be observed

between the temperatures of the two models. In conclusion, the temperature of the 0D model is not tracking properly the temperature of the 1D model.

OD vs 1D comparison based on HVAC load

In this section, OD and 1D will be compared based on the HVAC load which is the amount of heating or cooling required to maintain the internal temperature of the building inside the comfortable temperature range during the working hours. To determine this heating or cooling load, an additional term (Q_{HVAC}) has been introduced in energy balance (*Equation 9*).

$$C\frac{\partial T}{\partial t} = Q_c + Q_v + Q_r + Q_{int} + Q_{HVAC} \qquad \textit{Equation 9}$$

Regarding comfortable temperature, ASHRAE standard 55-2017, Thermal Environmental Conditions for Human Occupancy, provides guidelines about thermal conditions for human comfort. The temperature between 22-27°C is the range where most of the people neither feel hot nor cold [10]. Therefore, in this project, 22.5°C with tolerance of 2.5°C is considered as comfortable temperature range (20-25°C) to be maintained throughout the year for human comfort. Further details about HVAC control strategy to maintain the comfortable temperature can be found in appendix B.

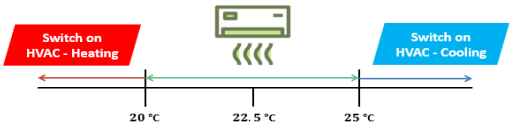

Figure 10: Comfortable Temperature Range

~~$C\frac{\partial T}{\partial t} = Q_c + Q_v + Q_r + Q_{int} + Q_{HVAC}$~~ ~~*Equation 9*~~

~~Regarding comfortable temperature, ASHRAE standard 55-2017, Thermal Environmental Conditions for Human Occupancy, provides guidelines about thermal conditions for human comfort. The temperature between 22-27°C is the range where most of the people neither feel hot nor cold [8]. Therefore, in this project, 22.5°C with tolerance of 2.5°C is considered as comfortable temperature range (20-25°C) to be maintained throughout the year for human comfort.~~

~~*Figure Comfortable Temperature Range*~~

~~In the case of OD, this Equation 9 is applied on the whole building, as it considered to be a single control volume and HVAC of load of whole building is calculated. However, in the case of 1D, this equation is applied on each and respective HVAC load of each room is calculated separately. Finally, the total HVAC of both models are compared and the model with higher fidelity has been selected for further analysis. The control strategy for HVAC in the code is shown in the Figure 14.~~

Field Code Changed

- ~~The model first loads the building specifications and weather data. It then checks for the hour of day.~~
- ~~If the current hour is inside the working hours, it checks for the current internal temperature (temperature of whole building in case of OD and temperature of respective room in case of 1D). If not, it keeps/switches the HVAC equipment off.~~
- ~~If the current temperature is inside the comfortable temperature range, it keeps/switches off the HVAC equipment. However, if not comfortable, it keeps/switches the HVAC equipment on.~~

- ~~Finally, how much HVAC load required to maintain the temperature is calculated. Three possibilities can be observed for HVAC load shown below.~~

$$\begin{cases} Q_{HVAC} > 0\ (Heating), & if\ T_{int} < T_{comfortable} \\ Q_{HVAC} = 0, & if\ T_{int} = T_{comfortable} \\ Q_{HVAC} < 0\ (Cooling), & if\ T_{int} > T_{comfortable} \end{cases}$$

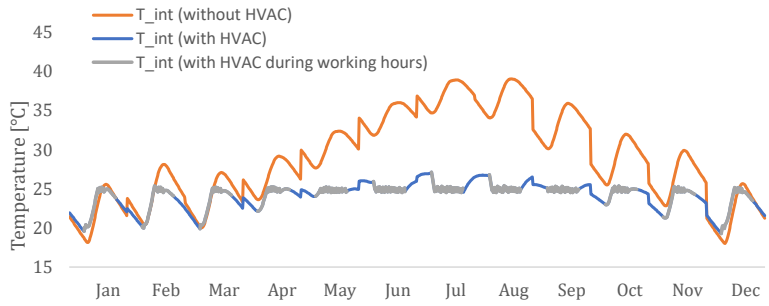

Figure 11 Temperature evolution of Room 11 with and without HVAC

Field Code Changed

Field Code Changed

Figure 11 shows the temperature evolution of room 11 from 1D model with and without HVAC as an example to demonstrate the working of control strategy applied for HVAC. It can be observed that HVAC equipment tries to maintain the temperature inside the comfortable temperature range during working hours, making the control volume a comfortable space for human. Therefore, it can be concluded that the control strategy is working as intended and results obtained for Q_{HVAC} can be used to compare OD and 1D models.

Results and Discussion: Comparison of HVAC load of OD and 1D is shown in **Error! Reference source not found.**. The positive values of HVAC load represent heating while that are negative represent cooling. It can be observed that whether heating or cooling is required is correlated with the season. For instance, during winter there is only heating; during spring and fall there is both heating and cooling, and during summer there is only cooling. Compared to heating, we observe that cooling has bigger share which is obvious as Barcelona, Spain is in hot and humid region.

Commented [AP1]: Should we keep this?

Field Code Changed

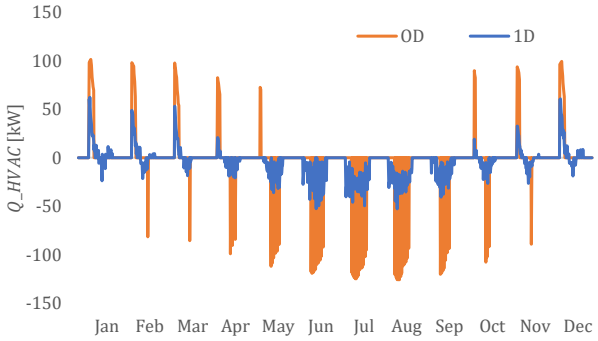

Figure 12: Comparison of monthly HVAC load of OD and 1D

Comparing OD and 1D, it is apparent that HVAC load in the case of 1D is less than that of OD. On average, HVAC load in the case of 1D is reduced by factor of 2. For instance, the peak load in the case of OD is around 127 kW, while that of 1D is around 63 kW. The reduction in HVAC load in 1D is observed because, unlike OD where the total control volume needs to be considered for calculation of HVAC load, room 8 (garden) and 12 (staircase) are excluded in 1D for HVAC load calculation because they are not required to be conditioned. Consequently, a significant amount of control volume is being reduced for HVAC load calculation

in 1D. In addition, room 8 has also skylight which allows direct radiation from roof, making room 8 as one of the hottest rooms in the building. These are the two main factors that caused reduced HVAC load for 1D.

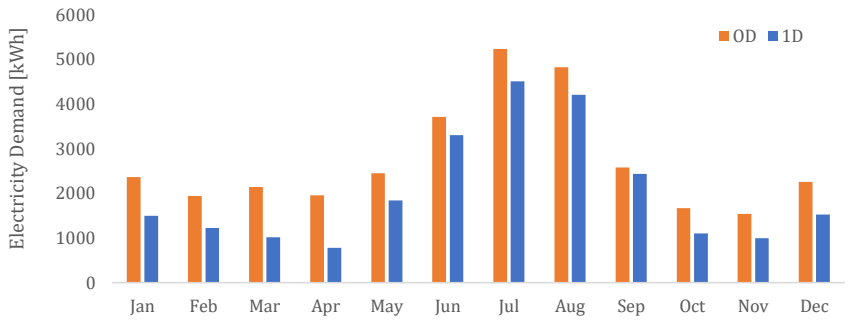

Figure 13: Electricity demand of heat pump

Field Code Changed

Field Code Changed

Figure 13 shows the monthly electrical energy demand of the heat pump. The bars in blue represents the electricity demand in case of OD, while that are shown in orange represents the electricity demand in case of 1D. A significant reduction in electricity demand for each month has been observed in case of 1D because of the same reasons explained for reduction in HVAC load. In case of OD, yearly electricity demand was calculated to be 32,686 kWh while that for 1D it was found to be 24,457 kWh, which translates into around 56% reduction in electricity demand.

Summary and Conclusion – OD vs 1D: Based on the results of HVAC load and electricity demand for OD and 1D models, it can be concluded that 1D is better than OD, as it provides accurate estimation of the peak HVAC load which in physical terms means the heat pump capacity and corresponding electricity consumption. Therefore, after this section of report, only 1D has been considered for further analysis including application of green building features and energy production plant.

Green building features

Elements incorporated in the building design or structure to minimize undesired heat gain or loss are called green building features. Before selecting a set of green building features for analysis, let's identify the heat sources that will allow us to reduce internal temperatures of the building. As discussed earlier, one of the major sources of heat gain in this case is radiation. While it is true that radiation helps in reducing the heating load in winter, its contribution to increasing the cooling load is huge. Therefore, it is necessary to implement a dynamic green building feature that allows us to take advantage of radiation in winter but at the time allow us to block the radiation in summer. Contrary to radiation, ventilation is the source of heat loss from the building. As already discussed in Figure 6, regardless of season, the internal temperature of the building is always higher compared to the external temperature. It implies that exchanging the inside air with outside air works as a free cooling, causing the internal temperature to reduce.

Considering the respective impact of radiation and ventilation on internal temperature of the building, two dynamic green building features are selected as follows for further analysis:

- Movable Curtains (MC)
- Demand Controlled Ventilation (DCV)

Movable Curtains: The feature of movable curtains is applied to all the rooms having glass wall on external side (opposite to the glass wall facing garden) to control the amount of radiation coming through the glazed walls. The feature works independently for each room to allow opening or closing of curtains depending on their internal temperature. The details on control strategy of movable curtains can be found in appendix B.

Impact on internal temperature:

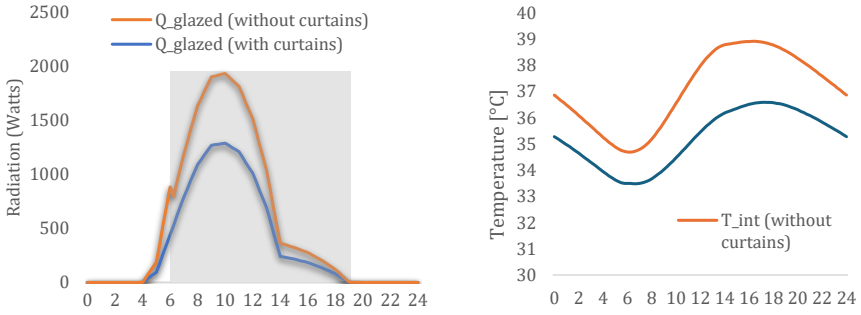

Figure 14: Impact of movable curtains on radiation and internal temperature of room # 11 in the month of July

Field Code Changed

Since the room # 11 is one of the hottest rooms, therefore, it is taken as an example to show the impact of applying movable curtains in the month of July in **Error! Reference source not found.**. The graph on the left shows the impact of movable curtains on radiation coming inside room # 11 with and without curtains. A significant reduction in incoming radiations and corresponding internal temperature shown on right can be observed after applying the movable curtains feature. Extending the approach to all months as shown in Figure 15, it can be observed that: firstly, there is no impact of movable curtains on winter months because the feature is not applied during these months to benefit from radiation. Secondly, a significant reduction in internal temperature is observed during summer months due to the blockage of relatively higher solar radiation during these months. Lastly, on average, applying the movable curtains can reduce the temperature by 2°C.

Field Code Changed

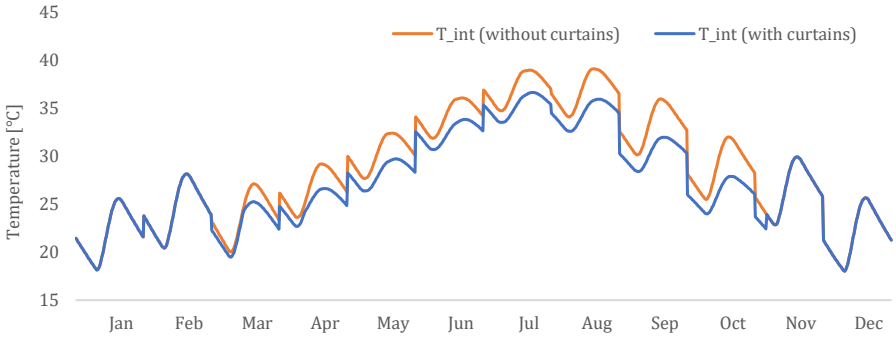

Figure 15: Year-round impact of movable curtains on internal temperature of room # 11

Field Code Changed

Impact on electricity demand:

In this section, impact of applying movable curtains on electricity demand of heat pump has been discussed. To visualize this impact, total electricity demand of the heat pump was determined with and without curtains using same approach shown in **Error! Reference source not found.** and following results were obtained. A significant reduction in electricity demand can be seen. It was determined that movable curtains reduce the yearly electricity demand from 24,457 kWh to 19,582 kWh which translates into reduction by 56% which demonstrates a remarkable potential of this feature to reduce energy consumption of buildings, especially in hot climates.

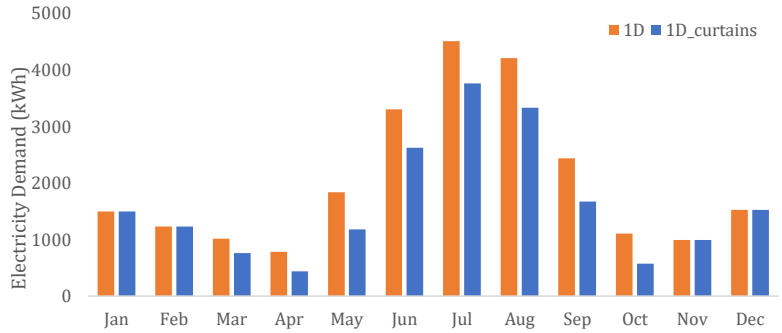

Figure 16: Impact of movable curtains on electricity demand

Field Code Changed

Demand Controlled Ventilation: This feature takes advantage of the fact that external temperature is lower than the internal temperature. Therefore, during working hours, when the internal temperature exceeds comfortable temperature, this feature increases the ventilation rate (n_{vent}) from 0.35 ACH to around 0.61 ACH (an increase of 75%) to provide free cooling effect. The tolerance and control strategy for this feature are same as that of discussed for movable curtains. The only differences are the control parameter which is n_{vent} in the case of DCV and it does not involve introduction of any new parameter in equation for ventilation shown in Equation 4, i.e., the mathematical expression does not change.

Impact on internal temperature:

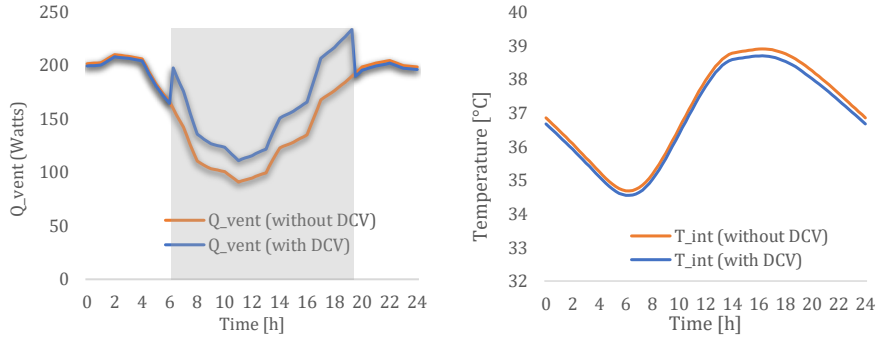

Figure 17: Impact of demand-controlled ventilation on ventilation and internal temperature of room # 11 in the month of July

Field Code Changed

Again, room # 11 and month of July are taken as an example to show the impact of demand-controlled ventilation on heat transfer through ventilation and the internal temperature in Figure 17. it can see in the graph on the left that during working hours, there is increase in heat transfer

Field Code Changed

to outside through ventilation in case of DCV compared to the case without DCV. Consequently, this impacted the internal temperature shown on the right and a slight decrease in temperature can be observed in case of DCV. Extending this approach to all months shown in Figure 18, it was found that applying the DCV feature can reduce the year-round average internal temperature less than 0.2°C only.

Field Code Changed

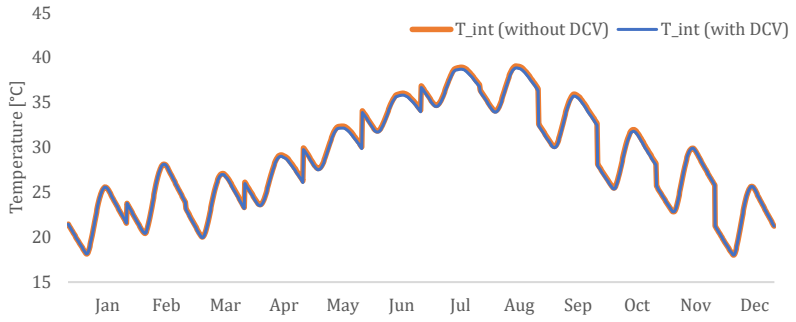

Figure 18: Year-round impact of DCV on internal temperature of room # 11

Field Code Changed

Impact on electricity demand:

To visualize the impact of DCV on electricity demand, the same approach was taken as of explained in case of movable curtains. Figure 19 shows the impact of applying DCV on electricity demand which shows no significant impact of this feature on electricity demand. It was found that applying this feature reduces the yearly electricity demand by only 30kWh which translates into reduction by 0.1% only.

Field Code Changed

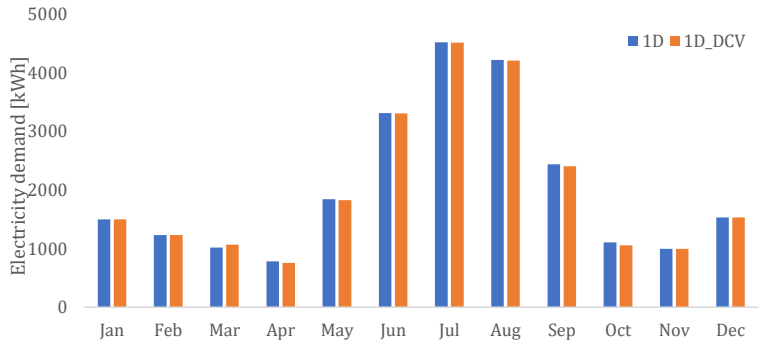

Figure 19: Impact of DCV on electricity demand

Field Code Changed

Summary - Movable Curtains vs Demand Controlled Ventilation: Feature of movable curtains and demand-controlled ventilation were selected for analysis. The impact of both features was observed on the internal temperature of rooms and the total electricity demand of heat pump. It was found that application of movable curtains can lead to reduction in average year-round internal temperature by 2°C, on the other hand, contribution of DCV is negligible, less than 0.2°C. Moreover, impact on electricity demand was also assessed and it was found employing movable curtains can reduce electricity demand by 56% while contribution of DCV is again negligible. It is concluded that movable curtains are better compared to DCV, therefore, only 1D model with movable curtains will be used for calculation of energy production plant.

Energy Production Plant Selection

Selection of the energy production plant is a delicate and highly important issue. The primary objective is to obtain the cheapest production system; however, the approach must also be environmentally viable and not only economically. This balance is crucial in creating a system that is both cost-effective and environmentally responsible, supporting long-term energy needs without compromising ecological integrity.

In the following chapters, the energy production plant selection, using thermo-economic assessment and environmental assessment will be thoroughly explained.

Electricity Driven Equipment vs Heat Driven Equipment

At the initiation of the project, there were two system proposals, an electricity driven system with PV panels and a heat pump, and a heat driven system, which consists of solar thermal collectors and an absorption chiller. After a thorough research and analysis, it was concluded that it is more viable do use electricity driven equipment for many reasons.

Firstly, PV panels are one of the most widely used energy resources in Spain and their availability is greater than that of solar thermal collectors. On the other hand, solar thermal collectors do have a higher efficiency, which ranges from 40% all the way up to 70%. Solar panels, on the other hand, have a maximum efficiency of around 20% . However, PV panels are much cheaper per area, and their prices range from 300 – 400 €/m², while solar thermal collector prices range from 800 – 1300 €/m². This huge price discrepancy is caused by multiple reasons. The price of PV panels has dropped by 65% during the last six years. Conversely, the price of the solar thermal collectors has risen since 2022 due to political reasons and stays higher in comparison to PV panels. Another advantage of PV panel system is that its operational expenditure and payback period are lower than that of the solar thermal collector system. Moreover, heat driven system requires thermal tanks and additional sources (e.g. gas burner) to cover peaks, which increases CO_2 emissions of the system significantly.

Commented [SS2]: https://www.ree.es/en/datos/generation/installed-capacity

Commented [SS3]: https://inaventasolar.com/en/case-studies/32-what-are-solar-collectors-and-are-these-different-from-solar-pv-panels

Commented [SS4]: UK, 2024, solarguide.co.uk Ireland, Sustainable Energy Authority of Ireland

Hence, it was decided to further examine electricity driven equipment, with PV panels and heat pump. In this research, it was dealt with two types of electricity driven equipment, which are, as it stands:

1. Stand-Alone System and
2. Grid-Connected System.

In the following chapters, the approach to the energy production plant selection, selection of the elements, the optimisation of the systems and results will be thoroughly explained.

Electricity Driven Equipment

1. System A: Stand-Alone System

The Stand-Alone System is an electricity driven system, which provides power to the HVAC system using electricity produced by PV panels and energy stored in the batteries. Battery storage is required to store electricity produced by the PV panels because solar power is intermittent. This system is not connected to the grid, hence the name *stand-alone*. The goal was to obtain an optimised stand-alone system, meaning an optimised number of PV panels and battery cells to minimise the investment cost. A simplified scheme of a stand-alone system that was used for the optimisation is presented in the figure below:

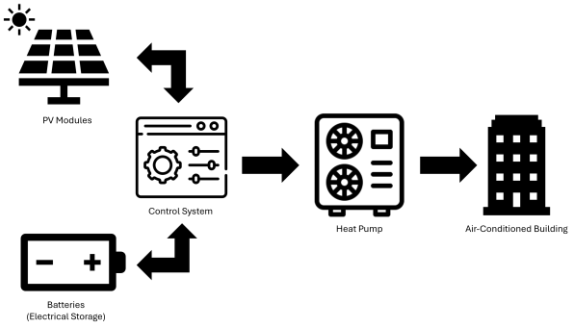

Figure 20 Stand-Alone system scheme

As it can be seen from the figure, the energy for the heat pump is supplied by the solar power converted into electricity by the PV panels and the energy stored in the batteries. Since the system is not connected to the grid, it is crucial to optimise it in a way that will ensure that the HVAC system is supplied by all times. Moreover, the system must be designed in such a way that it minimises investment costs. The biggest difference between the stand-alone and grid-connected systems is that the stand-alone system does not have operational expenditure i.e. the price paid for electricity imported from the grid.

Specifications of the Components of the Stand-Alone System

Before optimisation, it is important to define properties of components used in the given system. The data that will be presented in the following section was obtained via comprehensive research.

The cost of PV panels used in the system modelling is 850 €/kW of power. This price includes the installation costs and other components needed for the operation of PV panels. This data was obtained from *Statista* and is based on the installation costs of PV panels for the year 2022 [11].

The battery cells of the model are 360 VAh LiFePO4 batteries. The price of these batteries is 560 €/kWh [12], considering the lifespan of 20 years. The reasons why it was opted for these batteries is that they are lightweight, they are easy to transport and install, and are an ideal choice for outdoor installation. Moreover, Lithium-ion batteries are widely available and are usually the first choice for this purpose.

From the data that was obtained in the 1D analysis states that a 63 kW heat pump is needed. The heat pump that is recommended using is the air-to-air heat pump since it is suitable for the climate it will operate in. The coefficient of performance (COP) for heating is 3.23, while the COP for cooling is 2.23 [13].

Commented [SS5]: https://www.statista.com/statistics/809796/global-solar-power-installation-cost-per-kilowatt/

Commented [SS6]: https://nozzler.io/eco-worthy-12v-30ah-lifepo4/

Commented [SS7]: https://rmi.org/why-heat-pumps-are-the-answer-to-heat-waves/

1.1 Optimisation of the Stand-Alone System

The optimisation of the system was conducted using MATLAB programming language and the Genetic Algorithm method to obtain the results. To implement this method, firstly, the optimisation of the system required modelling of its components first. To calculate power produced by the PV panels, the Equation in Appendix C was used:

The modelling of the battery cells required calculating the State of Charge (SOC) of the batteries, to properly meet the objective and the constraints. The mathematical expression used to calculate the battery SOC at a given moment is shown by the Equation in Appendix C:

For this optimisation case, a simplified modelling of converters was used. It was considered their efficiencies to be $\eta_{DCDC} = 0.95$ and $\eta_{ACDC} = 0.95$.

Commented [SS8]: https://thundersaidenergy.com/downloads/dc-dc-power-converters-efficiency-calculations/#:~:text=DC%2DDC%20power%20converters%20are,are%20higher%20at%20low%20loads. https://www.renesas.com/us/en/products/power-power-management/acdc-isolated-dcdc-converters?gad_source=1

After the modelling of the components and proposing energy production functions, it was proceeded with the definition of variables, which are to be optimised by the Genetic Algorithm. For the stand-alone system, there are three variables:

1. N_{PV} – Number of PV panels
2. N_{Cell} – Number of battery cells of the proposed capacity
3. SOC_{ini} – the initial state of charge of the electricity storage.

Mathematically, it can be written as is described by the Equation in Appendix C.

After defining the variables which are to be optimised, it is to define the objective of the optimisation problem. The objective of the optimisation problem was to minimise the investment cost, which is crucial for the thermos-economic assessment. Mathematically, it is written as described by the Equation in Appendix C.

The final step of the optimisation problem is to define the constraints of the system. As mentioned in the introduction, for the Stand-Alone system, it is crucial for it to be supplied at any given moment, since it is not connected to the grid and relies solely on the energy produced by the PV panels and the energy stored in the battery cells. Hence, one of the constraints is $P_{unsup}(x,t) = 0, \forall\ t\ \in Observed\ interval$, which optimises the system in such a way that it always provides energy to the heat pump. Moreover, the lower and upper bounds of the variables dictate the minimum and maximum values of the optimised variable. For PV panels, the upper bound is the maximum number of PV panels that can fit the designated area. The lower and upper bounds of the SOC are constrained so that the battery system does not lose its performance throughout lifetime. And finally, the final state of charge should be greater of equal to the initial state of charge. The mathematical formulation of these constraints is represented by the Equation in the Appendix C:

Finally, the Genetic Algorithm can be implemented, and the results can be obtained. The results are presented in the following section. This optimisation approach can also be presented graphically. The Figure C.1 in the Appendix C represents the flowchart for the stand-alone system optimisation Approach.

1.2 Results of the Optimisation of the Stand-Alone System

After running the code, the optimisation results were as following:

N_{PV} – 43 panels
N_{Cell} – 200
SOC_{ini} – 77%

From the obtained results, it can be concluded that the system respected constraints and upper and lower bounds. The results of the energy production are presented in the following figure:

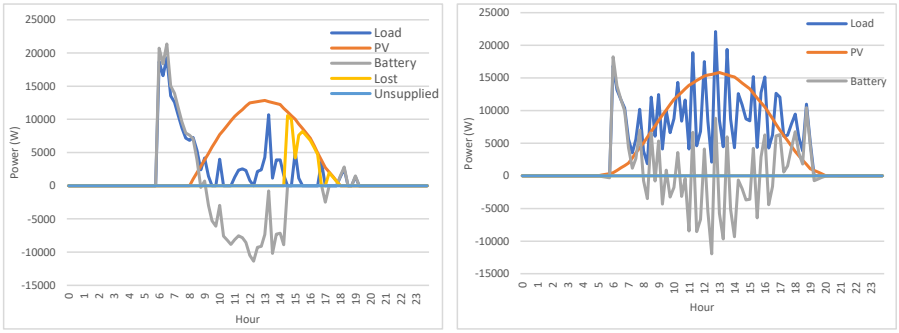

a) b)

Figure 21 Optimisation results of the Stand-Alone System for an average day in a) January and b) July

Error! Reference source not found. represents results obtained for the months of January and July, since those are the coldest and hottest month on average, respectively. The biggest observable difference between July and January is that there is no lost energy in July, while some energy is lost in January. The reason for this is that the load is much bigger in July, as cooling load is great. The system tends to store all the available, unused energy in the batteries, so it could be used later, as there are more sunny days in summer, hence higher PV production in July. Moreover, it can be seen that there was no unsupplied power in both cases, meaning that our system respected the defined constraints.

2. System B: Grid-Connected System

The Grid-Connected systems, like the stand-alone system is an electricity driven system which provides energy to the HVAC system of the building. Unlike the stand-alone system, the grid-connected system does not store electricity and uses electricity imported from the grid instead. Moreover, this system configuration has the option of selling excess energy.

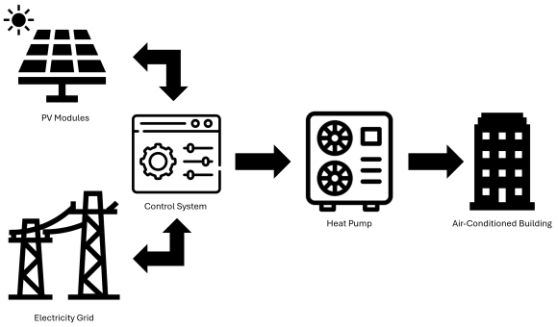

Figure 22 Grid-Connected system scheme

Specifications of the Components of the Grid-Connected System

For the grid-connected system, it was considered that the installation cost of PV panels is 850 €/kW as per *Statista*. This is the same price that was used for the stand-alone system, since there are no obvious reason to change the type of PV panels used in the production.

The heat pump used in this system is the same as the heat pump used for the stand-alone system, an air-to-air heat pump, suitable for hot climate, with a heating COP of 3.23 and cooling COP of 2.23.

What distinguishes the grid-connected system from the stand-alone system is the grid connection. Now, instead of electricity storage the electricity is directly imported from the grid. The import price of electricity is 0.281 €/kWh, taken as an average of the electricity price in Spain for the last two years. The electricity export price used in our optimisation is 0.02 €/kWh.

Commented [SS9]: https://countryeconomy.com/energy-and-environment/electricity-price-household/spain

Commented [SS10]: https://countryeconomy.com/energy-and-environment/electricity-price-household/spain

2.1 Optimisation of the Grid-Connected System

The optimisation of the Grid-Connected System follows a similar approach as the optimisation of the Stand-Alone System. The MATLAB programming language was used again as well as the Genetic Algorithm method. Firstly, the PV panel energy production was modelled, as per the same approach used for the stand-alone system, described by Equation in Appendix C.

After the modelling of PV panel production, the converters were modelled. In this system, a simplified modelling of converters was used, as in the previous case. It was considered that their efficiencies are $\eta_{ACAC} = 0.9$ and $\eta_{ACDC} = 0.91$.

Commented [SS11]: https://www.eurocomposant.fr/s/product/tn1500212b/01t3X00000IZPqjQAH?language=fr
https://assets.new.siemens.com/siemens/assets/api/uuid:3c5fe93a-be71-4d5c-b51d-a70199dba2b6/dfmc-b10032-00brsinamicsenus-72.pdf

The only optimised variable of this system is the number of PV panels, and its mathematical expression can be found in Equation in Appendix C. The algorithm tries to obtain an optimised number of PV panels, trying to minimise capital costs, but also produce enough electricity via PV panels to reduce the operational costs.

Unlike the optimisation problem of the Stand-Alone system, where one the system constraints was that the electrical load was supplied at all times, it was unnecessary here, since it was considered that the system can be supplied by electricity from the grid at any times, whenever it was needed (i.e. when there is no production by the PV panels). Hence, the objective of the problem is to minimise the cost, which now consists of both the capital and operational expenditures, since the system exchanges energy with the grid. The mathematical explanation of this objective is represented by Equation in Appendix C.

The constraints of this system are the lower and upper bounds of the number of PV panels, where the upper bound is the maximum number of PV panels that can fit the designated area:

$$Constraints = x^l \leq x \leq x^u$$

This optimisation algorithm of the grid-connected system is shown in Figure in Appendix C.

2.2 Results of the Optimisation of the Grid-Connected System

The final optimisation solution for the grid-connected system states that the optimum number of PV panels is **92**. The energy production results, captured for the months of January and July are represented in the following figure:

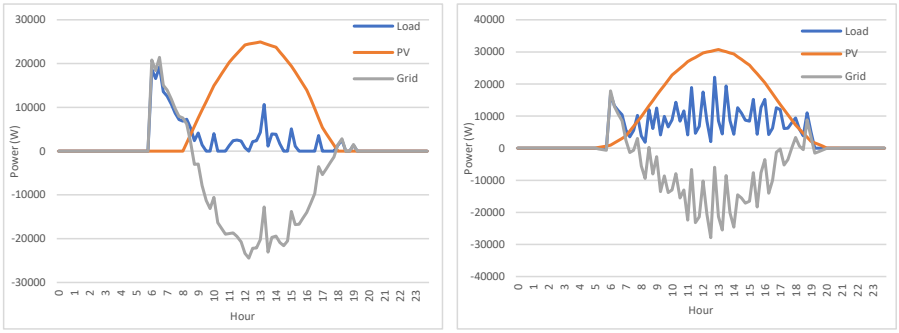

a) b)

Figure 23 Optimisation results of the Grid-Connected System for an average day in a) January and b) July

Similarly to the stand-alone system, the months of January and July were taken into consideration, as the coldest and hottest month of the year. The system is considered to supply the energy to the HVAC system all the time, since it is connected to the grid and is not constrained as the stand-alone system. From the results, it can be seen that when there is excess PV electricity production, it is sold to the grid. Conversely, if the PV electricity production is lower than the load demand, then the system buys electricity from the grid. This is clearly observable early in the morning, when the system has electrical load but since there is no sun energy, the system is forced to buy electricity from the grid.

Economic Comparison of the Stand-Alone and the Grid-Connected System

The results of optimisation for the stand-alone and the grid-connected systems obtained in the previous sections are used to economically compare the two named systems. The comparison between the Levelized Costs of Energy and the Payback period was used as means of the economic assessment.

Levelized Cost of Energy

The levelized cost of energy sets to compare the cost of energy per unit (kWh) with the traditional, grid-electricity-driven system.

$$LCOE = \frac{Total\ Lifetime\ Cost}{Total\ Energy\ Consumption}$$

The total lifetime cost is the sum of the capital and operational expenditures:

$$Total\ Lifetime\ Cost = Capex + Opex$$

The total lifetime cost of the Stand-Alone system is the investment cost of the PV panels and battery cells:

$$Total\ Lifetime\ Cost_{Stand-Alone} = Cost_{PV} \cdot N_{PV} + Cost_{Bat} \cdot N_{Bat}$$

The total lifetime cost of the Grid-Connected System is the sum of the investment cost of PV panels and the operational costs during lifetime:

$$Total\ Lifetime\ Cost_{Grid-Connected} = Cost_{PV} \cdot N_{PV} + Opex$$

The total electricity consumption for the lifetime of 20 years for both systems is obtained by the MATLAB optimisation code.

Payback Period

The payback period is calculated as

$$Payback\ Period = \frac{Total\ Cost\ of\ Initial\ Investment}{Cost\ of\ Annual\ Energy\ Import\ from\ the\ Grid}$$

The final results of the economic assessment for these two systems are

	Stand-Alone	**Grid-Connected**
CAPEX [€]	56 585	34 700
OPEX [€]	0	9 200
Total Lifetime Cost [€]	56 585	**43 900**
LCOE [€/kWh]	0.15	**0.11**
Payback Period	10	**7**

Table 2 Results of the economical assessment for both systems

Comparing these results with the price of electricity in Spain, which is 0.281 € / kWh, it can be concluded that both systems are cheaper per unit of energy compared to the traditional grid electricity supply. However, comparing the two given systems, the grid-connected system wins in all economic analysis. Firstly, its lifetime cost is cheaper than that of the stand-alone system, as is its Levelized Cost of Energy. Finally, the payback period is shorter for the grid-connected system, seven compared to stand-alone system's ten years. High investment costs are the main reason why the stand-alone system is less economically suitable than the grid-connected system. Furthermore, the grid-connected system can sell electricity to the grid, which lowers its operational costs. Hypothetically speaking, there is a certain optimisation point for which the total lifetime cost of the grid-connected system is zero, meaning that the system sells enough electricity to cover the capital expenditure.

Commented [SS12]: Reference from above

In conclusion, the thermo-economic assessment has shown that the more economically rentable system is the grid-connected system, as it beats the stand-alone system in every economic aspect. Its total lifetime cost is lower, as well as its levelized cost of electricity. Its shorter payback period makes it a perfect candidate from an economic point of view. However, apart from the economic benefits, the system should also be environmentally suitable for application according to modern standards. The following chapter will describe a detailed Life Cycle Analysis of the given systems, used to determine which system is more economically suitable. Combining the thermos-economic and environmental analyses, we will be able to determine the optimised system which meets both the economic and environmental requirements.

Technical and Environmental Assessment

Besides reducing power consumption, the major goal of this project is to decrease greenhouse gas emissions (GHG). A comprehensive environmental assessment of the building equipped with PV solar panels and a grid-connected system is critical to understanding its environmental impact. At present, Life cycle analysis (LCA) is the most commonly used tool to evaluate the impact of the system in every stage of life. In order to know the total emissions throughout its lifespan and the detrimental effect on the environment also on human health LCA is necessary.

Spain has set ambitious climate goals to address its greenhouse gas emissions and transition towards a sustainable energy system. Within 2030 reducing the emission by 23 % compared to 1990 heading toward net zero carbon emission in 2050 [14]. Thus, it is very important to perform life cycle analysis for different energy systems to understand the quantity as well as the sector where most of the emissions are coming out.

Additionally, technical assessments such as new components that are under development, and new technologies that could be used near future are also vital to understand the trend. Moreover, energy prices and other components' trends or forecasts have to be monitored to optimize the system. When in the near future advanced components will be available in the market, that could be utilized to retrofit the systems to get more advantage.

Life Cycle Assessment:

In the life cycle analysis, we compare the Standalone system and grid-connected PV with the conventional grid connection system. Here, in our case cradle-to-grave boundary systems are considered. 1KWh energy generation in 1 year is taken as a functional unit.

Stand-alone system:

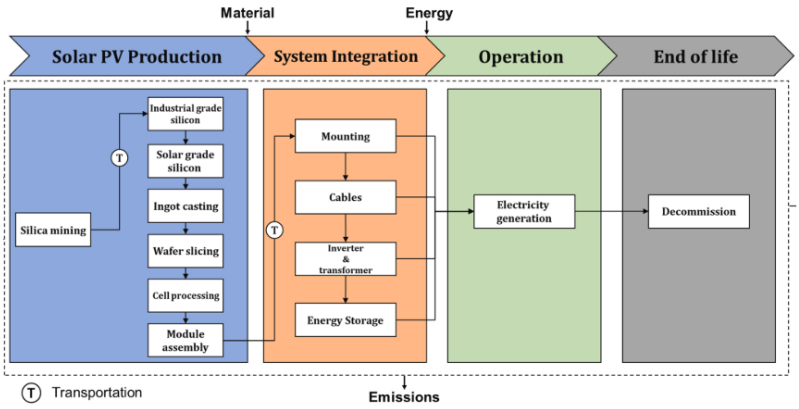

Fig 1 : Stand-alone system life cycle stages *[15]*

This **Error! Reference source not found.** depicts the cradle-to-grave system boundary considered in the study. The boundary includes the upstream processes of extracting silicon ore from mines. The energy and material requirements as well as raw material transportation in each step are considered in creating the life cycle inventory. In terms of transportation, both domestic ground and international maritime transportation are considered. For the "balance of system," the following major equipment types were considered: inverters, mounting structures, transformers, and physical infrastructures required for operation and maintenance. The life cycle GHG emissions range from 98.3 to 149.3 gCO2 eq /kWh with a mean value of 123.8g CO2 eq/kWh. The largest GHG emissions contribution is due to battery manufacturing, which accounts for 54% of the total. Lithium mining is quite energy intensive and anode binders emit high global warming potential gases. The second largest GHG emissions are from the production phase of solar PV panels [15].

Grid Connected PV:

In this system, there is no storage system only the PV panel is producing power. When there is a shortage of power, the grid will supply and when there is excess power from PV, it will go to the grid. Therefore, PV panel lifecycle and Spanish grid CO_2 intensity analysis are necessary here.

PV panel:

There are 3 major stages here upstream process, operational process, and downstream process. In the upstream process, raw material extraction, module manufacture, and installation. In 2nd stage, the operational phase is power generation, maintenance, and finally disposal of these panels. The National Renewable Energy Laboratory (NREL) led the Life Cycle Assessment of PV panels, and they found the GHG emission is around 40g/KWh CO_2 eq. [16]. Technological developments and different sustainable methods are helping to reduce this emission lower day by day.

Spain Electricity Mix:

In Spain, around 53% of electricity comes from renewable sources which makes them one of the lowest emission countries in the world. In every KWh energy generation, 160g CO2 equivalent is emitted. In *Fig: 5* we can see a significant amount of energy is coming from solar, wind, hydro, and nuclear. The emission from sources is quite low except from gas. Gas contributes huge amounts of emissions in Spain [17].In appendix D fig xxx shows the electricity mix of spain and sources of consumption as well as the GHG emission

Calculation of GHG Emission:

Table *3*, describes the comparison of 3 system's yearly GHG emissions in terms of CO_2 equivalent. Here, it is clearly understood that Grid-connected PV has negative emissions due to the significant amount of energy being exported to the grid, which will reduce the GHG emission of the grid. Around 5 tonnes of CO_2 eq gas will be reduced from the environment in 1 year. For the stand-alone system, 4.5 tonnes CO_2 eq will be added to the environment. Also, if we take the electricity solely from the conventional grid, it will add 3.1 tonnes of CO_2 eq in 1 year. So, in our case, a Grid-connected with a PV system is the most suitable choice.

Table 3: Comparision of GHG emission in 1 year

System type		Energy Generation (KWh)	GHG/Unit (Kg CO2 Eq)	Emission (Kg CO2 Eq)
Stand-Alone		36577	0.123	4528
Grid Connected PV	PV panel	71018	0.04	2840
	Import	5541	0.160	886
	Export	54859	0.160	-8777
	Total			-5050
Conventional Grid		19530	0.160	3124

Life Cycle Impact Assessment (LCIA):

LCIA provides a detailed understanding of the environmental impacts of the production, use, and disposal of the systems. It covers a wide range of impact categories, such as global warming

potential, ozone depletion, acidification, eutrophication, and resource depletion. This comprehensive analysis ensures that all potential environmental impacts are considered. In LCIA, mid-point and end-point impact categories are important to understand the intermediate and ultimate effects of a product or process on the environment. In Appendix D, table xx shows two impact categories of the PV system. There are four end impacts: resource depletion, climate change, eco-system and human health. Battery mainly affects resources and human health whereas PV mostly affects climate change. Other accessories affect the eco-system significantly.

Maintenance needs, Risk Assessment, and Viability

Both energy production plant options require extra calculation in terms of maintenance need, risk assessment, and viability to determine the suitability of the system specifically in longer run.

Aspect	**Standalone System**	**Connected to the Grid System**
Viability	Higher installation cost due to extra component (battery) Operational cost could be considered as zero. Full independence on power production, very beneficial for remote areas. Limited scalability.	Lower installation cost. Higher expected operational cost, however, with a possibility to sell excess energy to the grid. Grid reliance for backup. Easier scalability with grid support.
Maintenance Needs	PV Panels and Heat Pumps have to be maintained regularly. Extra maintenance is needed for the battery storage system (cells and inverters).	PV Panels and Heat Pumps have to be maintained regularly. Must be able to comply to the grid regulations/standards.
Risk Assessment	System is weather-dependent, no backup system if the PV cannot produce power in a long period. Extra risk on battery's reliability	In a big city as Barcelona, lower power outage risks could be expected. System does not have battery.

Comparing both systems in terms of viability, maintenance needs, and risk assessment, on top of economic and environmental assessment, connected to grid systems would be a better fit for the currently studied office area in Barcelona, Spain.

Potential Improvements in the Near Future:

Solar Panel Efficiency improvements

First-generation solar cells are used worl [14]dwide, and these have the highest commercial efficiency. Currently, the efficiency varies from 15-23% for residential systems. Single crystalline solar cells, Polycrystalline solar cells are mostly used. Second-generation solar cell Technology (Thin film solar cell technology) Si crystal wafer technology is costly as it uses mostly pure crystalline Si. Third-generation PV cell technology refers to single junction solar cells that can overcome the Shockley– Queisser limit of 31–41% power efficiency [18]. Perovskite solar cell technology is developing rapidly, it could be a potential solution for the low efficiency of current solar cells in the market. These cells offer a cheaper and more efficient alternative to traditional silicon cells, dramatically increasing the accessibility and efficiency of solar power. It is expected that a 4T perovskite–silicon tandem solar cell can achieve an efficiency of 26% or even beyond 26% in the laboratory followed by a 2T perovskite–silicon cell by the year 2025. Figure*Fig 2* shows how the solar cell efficiency varies over time. It is showed that crystalline solar cells efficiency is increasing slowly while emerging PV is increasing rapidly within some years.

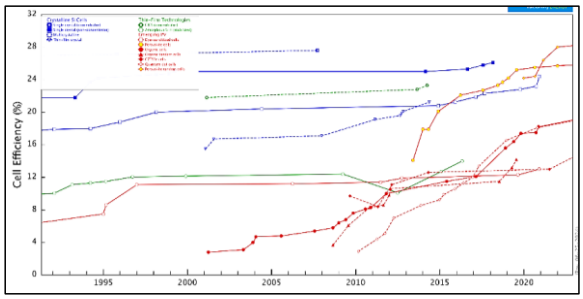

Fig 2: Trends in solar cell efficiency over time *[19]*

Transparent solar panels

Another strategy could be effective to use solar panels integrated with the building. Transparent solar panels represent a significant innovation, particularly for Building integrated photovoltaics (BIPV).The selective absorption enables the panels to generate electricity without obstructing visibility. These panels can be integrated into windows and glass surfaces, opening up new avenues for solar energy harvesting in buildings without compromising on aesthetics.

Bifacial Solar cells:

Passivated Emitter Rear Cell (PERC) is an advanced kind of solar cell technology that could give more efficiency. Bifacial solar cells can generate electricity not only from the sunlight incident on the front surface of a solar cell but also from reflected sunlight at the rear part.

Prices Evolution for Energy and Components

Electricity price:

Spain is making significant progress in transitioning to a clean and sustainable electricity sector 53% of energy is coming from the renewables sector. In the near future trend shows that electricity prices will decrease substantially. It will positively affect the operational cost of the system. Moreover, lower electricity prices reduce the immediate financial savings that homeowners achieve by generating their own power, as the cost offset from solar energy will be smaller. This can lead to a longer payback period for the initial investment in PV systems.

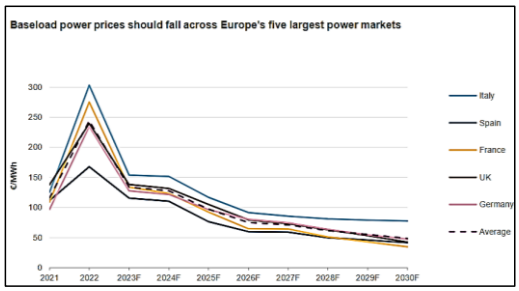

Fig 3: Energy price forecast [5]

Battery price:

Lithium-ion battery prices will also drop. It will reduce the capital expenditure of the system. With cheaper batteries, households can increase their storage capacity, ensuring a reliable power supply even during night-time or cloudy days when solar generation is low. It will also reduce the dependency on national grid. In addition to, more advanced Li-ion battery will come out in future that will also increase the charging-discharging capacity.

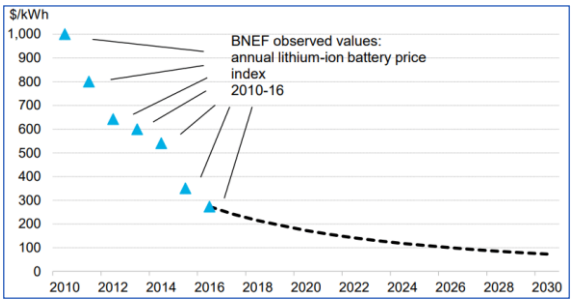

Fig 4: Lithium-ion battery price forecast [6]

Conclusion

Future Work

Appendix C

The model for calculation of power produced by PV panels is:

$$P_{PV} = N_{PV} \cdot \eta_{PV} \cdot P_{STC} \cdot \frac{GSR(t)}{G_{STC}} \cdot \left(1 - C_T(T(t) - T_{STV})\right)$$

where: N_{PV} is the number of PV panels; η_{PV} – PV panel electrical efficiency; P_{STC} – nominal power under Standard Test Conditions (STC); G_{STC} – STC Global Solar Radiation (1kW); C_T – temperature coefficient; T_{STC} – STC temperature (℃). $GSR\,(t)$ and $T(t)$ data were obtained from the *Photovoltaic Geographical Information System* from the European Commission (reference).

Commented [SS13]: PVGIS

The calculation of the battery system state of charge is calculated based on the following equation:

$$SOC(t + \Delta t) = SOC(t) - \eta_{Bat} \cdot \frac{P_{Bat}}{N_{Cell} \cdot C_{Cell}} \cdot \Delta t$$

where: SOC – battery state of charge; η_{Bat} – battery efficiency; P_{Bat} – battery power; N_{Cell} – number of cells; C_{Cell} – cell capacity. The battery SOC is constrained, which will be explained in the following paragraphs.

The mathematical representation of the stand-alone system variables is

$$x = (N_{PV}\ N_{Cell}\ SOC_{ini}) \in \mathbb{N}^2 \times \mathbb{R}$$

Mathematical representation of the stand-alone system optimization objective:

$$\min_x Cost^{inv}(x)$$

where

$$Cost^{inv} = Cost_{PV} \cdot N_{PV} + Cost_{Bat} \cdot N_{Bat}$$

and $Cost^{inv}$- Investment cost; $Cost_{PV}$ – Investment cost of PV panels (per power); $Cost_{Bat}$ – Investment cost of battery storage (per energy capacity).

The mathematical representation of stand-alone system constraints is

$$Constraints = \begin{cases} x^l \le x \le x^u \\ SOC_{min} \le SOC(x,t) \le SOC_{max}, \forall\, t \in Observed\ interval \\ P_{unsup}(x,t) = 0, \forall\, t \in Observed\ interval \\ SOC(x, t_{final}) \ge SOC(x, t_{start}) \end{cases}$$

The algorithm of the stand-alone system optimization:

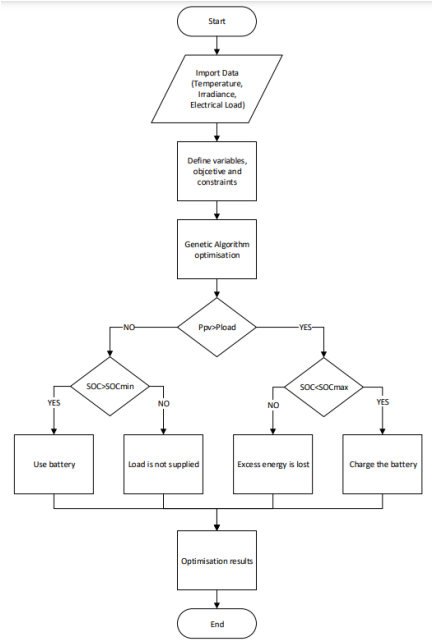

Figure 24 Stand-Alone System optimisation algorithm

The mathematical expression of the grid-connected system variable:

$$x = N_{PV} \in \mathbb{N}$$

The objective of the grid-connected system is

$$\min_{x} Cost(x)$$

where

$$Cost(x) = Capex(x) + Opex(x)$$

meaning that apart from the investment cost

$$Capex(x) = Cost_{PV} \cdot N_{PV}$$

there are also operational costs. $Opex(x)$, where x is the number of PV panels (N_{PV}) is calculated using a specially coded MATLAB function which calculates operational costs at each interval and then sums up the total operational expenditure for the observed period (in this case it is *1 year*).

The algorithm of the grid-connected system optimization:

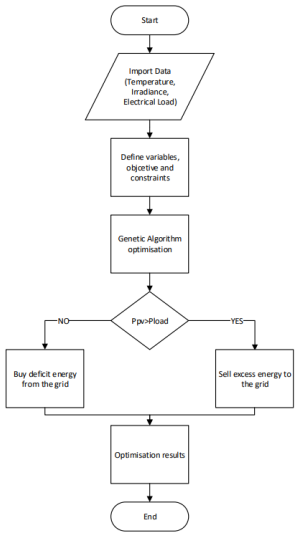

Figure 25 Grid-Connected System optimisation algorithm

APPEDIX D

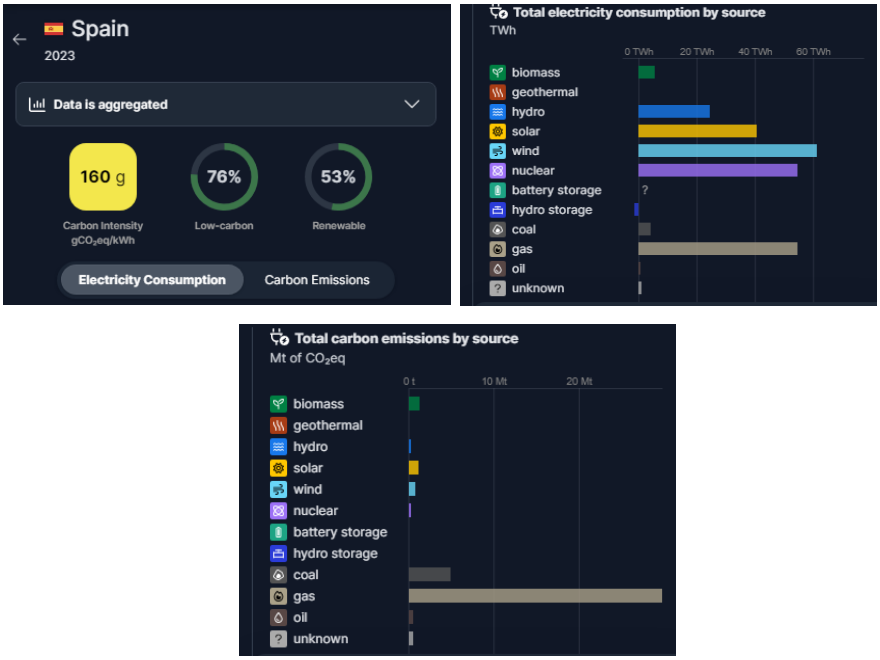

Fig: 5: Spain electricity mix and emission [2]

Table 4: LCA Impact Assessment [3]

Mid Point Impact	**End-point impact**
Fossil fuels	Resource
Minerals	
Global Warming	Climate change
Land Use	Eco-system
Eutrophication	
Minerals	
Carcinogen	
Ozone layer	
Radiation	
Acidification	
Radiation	Human health
Toxicity	
Oxidation	

Bibliography

Abir reference:

Appendix A : General Specifications

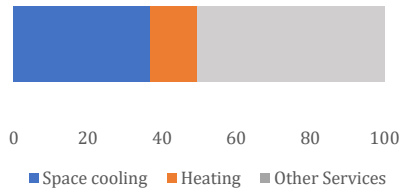

Figure 26 Share of Global Electricity Demand by 2050 [1]

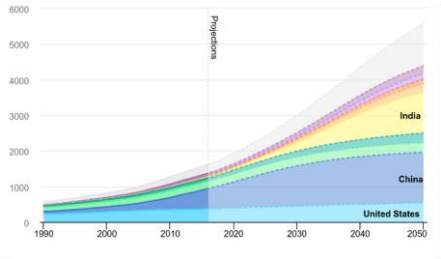

Figure 27 Expected AC Stock Growth by 2050 [1]

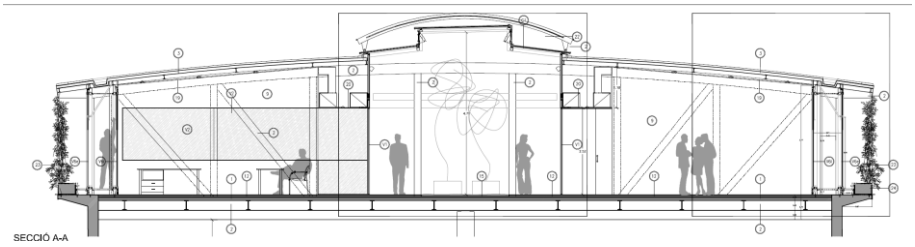

Figure 28 Cross Section of the Building [4]

Table 5 Building Materials and Dimensions

#	Layer Description	Material	Density [kg/m³]	Specific Heat [kJ/kg.K]	L [m]	λ [W/m.K]
		Superior Cover				
1	Sandwich cover	Prefabricated steel sheet	7800	0.9	0.001	60
	Vapor barrier	Polyethylene sheet	941	1.55	0.002	0.4
	Thermal Insulation	Rock wool	110	0.9	0.08	0.033
	Sandwich cover	Prefabricated steel sheet	7800	0.9	0.0006	60
		External Glass Facade				
2	External glass facade	Laminated Safety Glass	2480	1.9	0.02	1
		Internal Glass Facade				
3	a	Low emissivity glass	2500	0.84	0.008	1
	b	Air layer	1.225	1.005	0.012	0.026
	c	Low emissivity glass	2500	0.84	0.012	1
		Internal Glass Wall				
4	Internal glass wall (V1, facing corridor)	Laminated safety glass	2480	1.9	0.012	1
5	Internal glass wall (V2, facing adjacent rooms)	Laminated safety glass	2480	1.9	0.016	1
		Brick Wall				
6	Brick Wall	Brick	480	840	0.2	1
		Floor				
7	Floor	Corrugated sheet steel and concrete	1200	475	0.12	1.74

Appendix B: 0D and 1D Analysis

HVAC Control Strategy

In the case of OD, the Equation 9 is applied on the whole building, as it considered to be a single control volume and HVAC of load of whole building is calculated. However, in the case of 1D, this equation is applied on each and respective HVAC load of each room is calculated separately. Finally, the total HVAC of both models are compared and the model with higher fidelity has been selected for further analysis. The control strategy for HVAC in the code is shown in the **Error! Reference source not found.**.

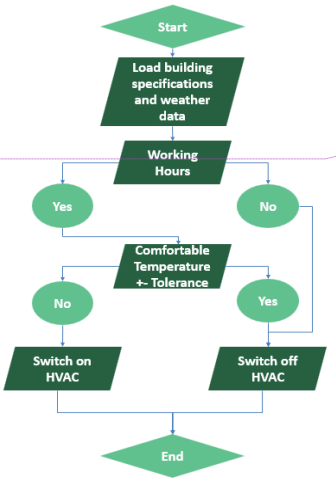

Figure 29: HVAC control strategy

- The model first loads the building specifications and weather data. It then checks for the hour of day.
- If the current hour is inside the working hours, it checks for the current internal temperature (temperature of whole building in case of OD and temperature of respective room in case of 1D). If not, it keeps/switches the HVAC equipment off.
- If the current temperature is inside the comfortable temperature range, it keeps/switches off the HVAC equipment. However, if not comfortable, it keeps/switches the HVAC equipment on.
- Finally, how much HVAC load required to maintain the temperature is calculated. Three possibilities can be observed for HVAC load shown below.

$$\begin{cases} Q_{HVAC} > 0\ (Heating), & if\ T_{int} < T_{comfortable} \\ Q_{HVAC} = 0, & if\ T_{int} = T_{comfortable} \\ Q_{HVAC} < 0\ (Cooling), & if\ T_{int} > T_{comfortable} \end{cases}$$

Energy Demand Calculation approach

Based on the results of HVAC load, monthly electricity demand of heat pump was calculated. To transform HVAC load into electricity demand, area under the curve was calculated which results in thermal energy demand which was further divided by the value coefficient of performance heat pump ($COP_{heat\ pump}$), as shown in **Error! Reference source not found.**. The $COP_{heat\ pump}$ depends on whether thermal energy demand is heating or cooling.

$$Electricity\ Demand\ [kWh] = \frac{\int Q_{HVAC}[kW]dt}{COP_{heat\ pump}} = \frac{Thermal\ Energy\ Demand\ [kWh]}{COP_{heat\ pump}}$$

Movable Curtains Control Strategy

The control strategy of movable curtains is like that of HVAC except that, unlike HVAC, there is only upper tolerance of 1.5°C and it only works if the internal temperature of the room exceeds the comfortable temperature range during spring, summer and fall because during winter radiation is beneficial for reducing the heating load. Mathematically, the implementation of movable curtains can be expressed as:

$$Q_{glazed} = f_{sh}\tau A_{glazed} G_{sun}(1 - f_{green\ facade})(1 - f_{curtains})$$

In nutshell, during the working hours, if the internal temperature of the room will go above comfortable temperature range (22.5-24°C), the curtains will close by 50% ($f_{curtains} = 0.5$), blocking the proportional amount of radiation.

Appendix C : Thermo-economic Assessment

Appendix D : Environmental Assessment